J. Phys. IV France **133** (2006) 355–360

DOI: 10.1051/jp4:2006133072

High energy electron transport in solids

R.B. Stephens[1], R.P.J. Snavely[2], Y. Aglitskii[11], K.U. Akli[4], F. Amiranoff[6], C. Andersen[4], D. Batani[7], S.D. Baton[6], T. Cowan[5], R.R. Freeman[3], J.S. Green[3], H. Habara[10], T. Hall[14], S.P. Hatchett[2], D.S. Hey[3], J.M. Hill[3], J.L. Kaae[1], M.H. Key[2], J.A. King[4], J.A. Koch[2], R. Kodama[9], M. Koenig[6], K. Krushelnick[8], K.L. Lancaster[10], A.J. MacKinnon[2], E. Martinolli[6], C.D. Murphy[10], M. Nakatsutsumi[9], P. Norreys[10], E. Perelli-Cippo[13], M. Rabec Le Gloahec[12], B. Remington[2], C. Rousseaux[12], J.J. Santos[6], F. Scianitti[13], C. Stoeckl[7], M. Tabak[2], K.A. Tanaka[9], W. Theobald[7], R. Town[2], T. Yabuuchi[9] and B. Zhang[4]

[1] *General Atomics, San Diego, CA, USA*
[2] *Lawrence Livermore National Lab., Livermore, CA, USA*
[3] *The Ohio State University, Columbus, OH, USA*
[4] *Department of Applied Sciences, University of California, Davis, CA, USA*
[5] *University of Nevada, Reno, NV, USA*
[6] *Laboratoire pour l´Utilisation des Lasers Intenses, CNRS-CEA Université Paris VI, École Polytechnique, 91128 Palaiseau, France*
[7] *Laboratory for Laser Energetics, Rochester, NY, USA*
[8] *Imperial College, London, UK*
[9] *Institute for Laser Engineering, Osaka, Japan*
[10] *Central Laser Research Facility, Rutherford-Appleton Lab, Chilton, UK*
[11] *Science Applications International Corporation, MacLean, VA, USA*
[12] *Commissariat à l´Énergie Atomique, 91680 Bruyères-le-Châtel, France*
[13] *Dipartimento di Fisica "G. Ochialini", Università degli Studi di Milano-Bicocca and INFM, Milan, Italy*
[14] *Department of Physics, University of Essex, Colchester, UK*

Abstract. With the addition of recent PW shots, the propagation of short-pulse laser generated electron beams have been studied using laser pulse energies from 30 J to 300 J, generating currents up to ∼15 MA in solid Al:Cu targets. This is ∼5% of the current that will be required in an ignition pulse. To this level, the current appears to simply scale with laser power, the propagation spread not change at all. The resistance of the aluminum does not seem to play a role in the propagation characteristics, though it might in setting the current starting parameters. We do find that at the highest currents parts of these targets reach temperatures high enough to modify the Cu-K_α emission spectrum rendering our Bragg imaging mirrors ineffective; spectrometers will be needed to collect data at these higher temperatures.

1. INTRODUCTION

A fast ignition target, after being compressed, is ignited with a short pulse of energy sufficient to raise the temperature of a minimum volume (ρR∼0.5) to ∼10 keV [1]. For fuel with $\rho \sim 200$/cc that requires ∼40 kJ of energy deposited in ∼15 ps, or ∼200 MA of 1 MeV electrons. A number of experiments have shown that the conversion efficiency of short-pulse light to energetic electrons is ∼30% [2, 3], so that

current requires $\sim$120 kJ/15 ps = 8 kJ/ps. The best lasers available at present can deliver $\sim$300 J/1 ps giving $\sim$5% of the required current.

Recently completed 300 J, 1 ps shots on the Vulcan PW laser at the Rutherford Appleton Lab have been combined with previous electron propagation investigations using $\sim$30 and 100 J laser pulses [4] to consider the scaling of electron propagation with increasing current. Over this range, we find that the current scales with laser energy, and the beam spread is independent of it. We also find that at these high energies the targets are reaching sufficiently high temperatures, especially on the laser side, as to render our Bragg imaging mirrors ineffective. We have therefore fielded high-resolution spectrometers as alternative (non-imaging) detectors.

2. EXPERIMENTAL SETUP

Current propagation was observed by using a Bragg mirror to image K_α fluorescence from a Cu fluor into an x-ray ccd camera. Three geometries were used (Fig. 1): 1) a $\sim$20 μm thick Cu layer buried at various distances from the laser-plasma interface and viewed through the back surface as described in [4]. 2) an Al:Cu alloy slab that was illuminated from a thin face, $\sim$50 μm from one edge and viewed from the side, and 3) a 20 μm diameter Cu wire coupled to the laser through a hollow Al cone.

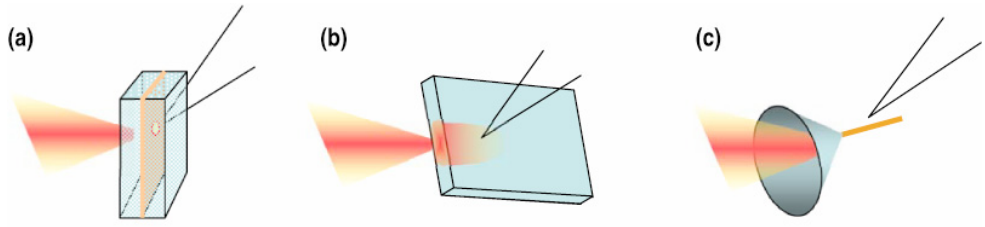

Figure 1. Experimental setup for transport experiments. (a) Aluminum slab with a buried 20 μm thick Cu layer viewed from the side away from the laser, (b) Al:Cu alloy viewed from the side, (c) 20 μm diameter Cu wire at the tip of an aluminum cone.

2.1 Buried layer slab geometry

Images from the slab geometry give the cross-section of the propagating electron beam at specific distances. The diameters obtained from the recent 300 J experiments are in excellent agreement with the previously published results from the lower energy shots [Fig. 2(a)]. The integrated intensity from these targets (normalized to laser energy) is also in good agreement [Fig. 2(b)], except for the thinnest target, which shows even less fluorescence than observed for more deeply buried Cu layers.

We expect that is a consequence of the narrow reflection bandwidth of the Bragg mirror, missing the emission band from the hot plasma. A FLYCHK [5] calculation of the expected emission and consequent detection efficiency as a function of temperature is shown in Fig. 3. The $\sim$3 eV bandwidth of the Bragg imaging mirror is the vertical line centered on one of the peaks of the cold Cu K_α emission. As the temperature rises above $\sim$10 eV, and the Cu ionizes, this line is replaced with emissions outside the reflection bandwidth and the fluorescence detection efficiency drops by an order of magnitude. Assuming that the 300 J pulse on the 20 μm thick Cu target raises the local temperature above 100 eV resolves the contradiction with the data from the more deeply buried layers, and leads to the conclusion that the normalize current from the 300 J pulse is about the same as from the 70 J pulse.

The propagation distance of these laser-generated electrons, measured by plotting the maximum intensity as a function of Cu layer depth, showed a 1/e distance of $\sim$70 μm.

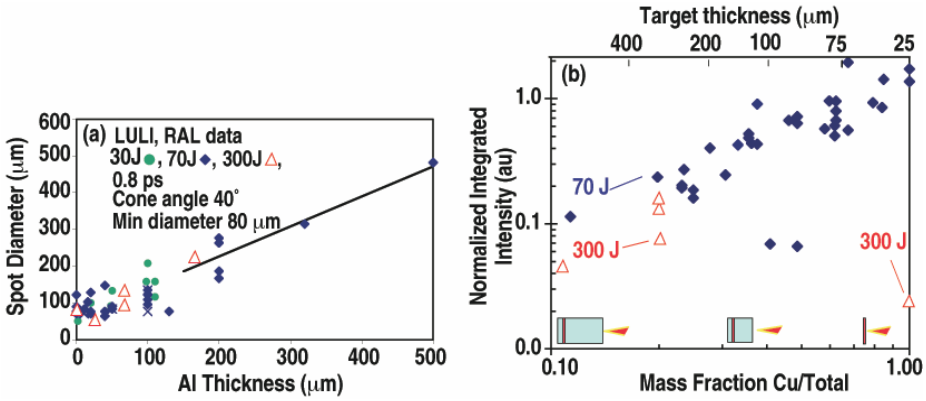

Figure 2. (a) FWHM spot diameter as a function of propagation distance in aluminum for 30 J (LULI - ●), 100 J (RAL – ♦ & 5's), and 300 J (RAL – △). b) Integrated K_α fluorescence intensity normalized to laser pulse energy as a function of the fraction of Cu in the target for 70 J (♦) and 300 J (△) shots.

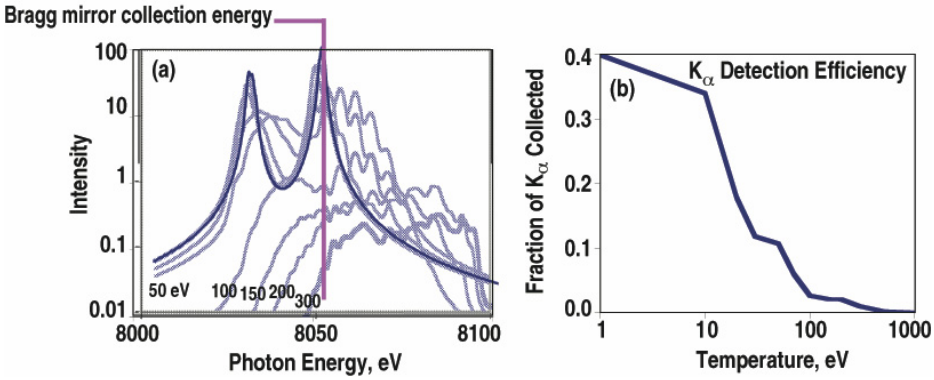

Figure 3. (a) A FLYCHK calculation of the K_α fluorescence emission spectrum as a function of temperature. The vertical line shows the reflectance band of the Bragg mirror used to image the fluorescence emission. (b) shows the detection efficiency of that mirror as a function of temperature.

2.2 Alloy slab geometry

The buried layer geometry discussed in Section 2.1 gives only one data point per experiment; shot-to-shot variations in the experiment (laser, target, diagnostic) add to the measurement noise. A side view of a Cu alloy slab [Fig. 4(a)] gives a view of the e beam propagation over its entire distance in one shot. The view one gets is analogous to that of the light from a passing car headlight on a foggy night. A very foggy night; the 1/e depth for fluorescence emission is only ∼50 μm. As a result the camera detects a thin slice of the expanding beam. Correcting for that expansion [Fig. 4(b)], one finds a mfp of ∼70 μm, as in the buried layer geometry.

2.3 Cone wire geometry

The cone-wire geometry shown in Fig. 1(c) gives yet another view of the electron propagation [Fig. 5(a)]. The hollow cone intercepts the entire laser beam and perhaps concentrates the resulting electron flux into a narrower area [6]. Electrons in the wire are then confined by electrostatic fields to a constant

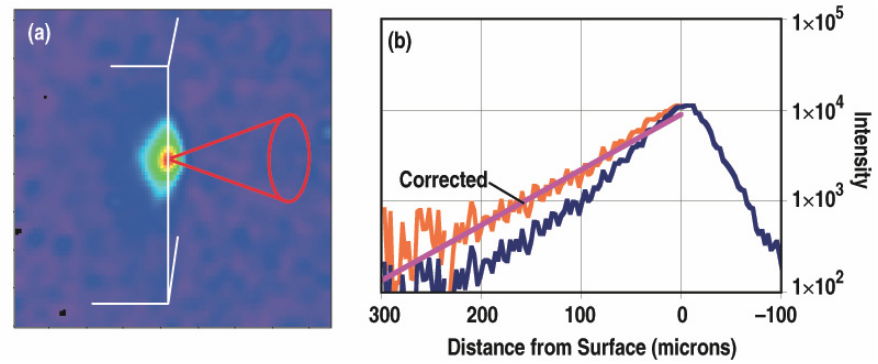

Figure 4. (a) Cu-K_α emission from the side of a $Cu_{0.4}Al_{0.6}$ alloy slab (edges indicated with white lines, laser focus with a red cone). (b) Fluorescence intensity as a function of distance from the laser along the slab surface as measured and corrected for expansion away from the surface. The corrected 1/e decay length is $\sim 70\,\mu$m.

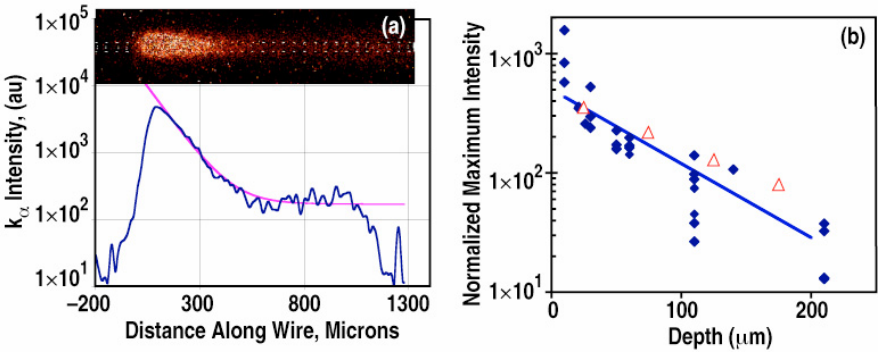

Figure 5. (a) Cu-K_α emission from the indicated region of a 20 μm diameter wire in the end of an Al cone. The exponential decay has a 1/e length of $\sim 100\,\mu$m. (b) Normalized K_α fluorescence intensity from the Cu wire (triangle) compared to earlier data from buried slab geometry [4].

$\sim 20\,\mu$m diameter. It appears that the normalized currents are very similar to that from the buried layer data [Fig. 5(b)]. The slight difference in slope (1/e length ~ 70, 100 μm for the slab and wire, respectively) is explained by the lack of spreading in the wire.

3. DISCUSSION

Although the current density carried by the wire, as measured by the maximum K_α intensity is the same in the slab, the fraction of the laser energy it carries is considerably reduced ($\sim 16\times$) because of the smaller diameter of the wire—closer to 2% than 30%; the current seems to be stopped in the cone rather than squeezing into the wire. This effect is in addition to any bottle-neck at the laser plasma interface [hinted at by the steep drop-off in the first few points of Fig. 5(a)]. Rather this limitation could be related to the reactive electric fields caused by large electrical resistance ($\sim 2 \times 10^{-6}\,\Omega$-m at 40 eV) of the aluminum [7]. The energetic electron current generated by the laser pulse (~ 10 MA from a 300 J pulse), although itself collisionless, is necessarily matched by a return current produced from the (relatively) cold plasma electrons. The potential driving that return current impedes the fast electrons (with distribution temperatures 300–800 eV [8]) and at high current densities that potential could completely stop the fast electrons. Figure 6 shows the expected fields and currents as a function of depth assuming Al resistance $2 \times 10^{-6}\,\Omega$-m, ion temperature 600 eV, and conversion efficiency 30%. For the conditions as observed

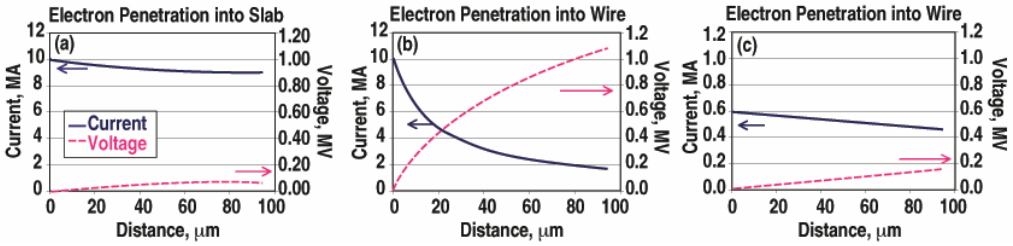

Figure 6. Calculated electron current and reactive potential as a function of penetration depth for (a) initial diameter and spreading in buried layer experiments, (b) the same current pushed into a wire with no spreading allowed, and c) the observed current traveling down a wire.

in the buried layer experiments, in which the current starts at 80 μm diameter and spreads at a 40° angle, the impeding potential is only a small fraction of the typical electron energy ($\sim$1 MeV), so very little current is lost in that case [Fig. 6(a)]. However, putting that same current into a 20 μm diameter wire, and not allowing any spread produces reactive fields that stop most of the electron current in $\sim$ 10 μm [Fig. 6(b)]. Matching the current density rather than the current results in potential fields that are again small [Fig. 6(c)].

The point of this analysis is just that understanding propagation in these shapes will require detailed understanding of the interaction of fields and currents in the region near the laser-plasma interface. By the time the diagnostics discussed here come to bear, such fields seem to be insignificant and, as observed earlier [4] a field-free Monte-Carlo model describes the propagation very well; the important field effects seem to be encapsulated in the heuristic rules used to generate the electrons. We can say from this analysis that those rules are not dependent on total pulse energy at least up to the level so far investigated. The normalized current, the propagation geometry (initial diameter and spreading angle) and the propagation length all remain constant over this range.

4. SUMMARY

With the addition of recent PW shots, the propagation of short-pulse laser generated electron beams have been studied using laser pulse energies from 30 J to 300 J, generating currents up to $\sim$15 MA in solid Al:Cu targets. This is $\sim$5% of the current that will be required in an ignition pulse. To this level, the current appears to simply scale with laser power, the propagation spread not change at all. The resistance of the aluminum does not seem to play a role in the propagation characteristics, though it might in setting the current starting parameters. We do find that at the highest currents parts of these targets reach temperatures high enough to modify the Cu-K_α emission spectrum rendering our Bragg imaging mirrors ineffective; spectrometers will be needed to collect data at these higher temperatures.

Acknowledgments

We gratefully acknowledge the target fabrication group at General Atomics, especially J. Smith, E. Giraldez, and C. Shearer, who developed and fabricated the complex target geometries used in these experiments. This work was supported under the auspices of the U.S. Department of Energy under contract No. DE-FG03-00SF2229; by the University of California, Lawrence Livermore National Laboratory under Contract No. W-7405-Eng-48; and with the additional support of the Ohio State University, the Hertz Foundation and General Atomics. The experiments were additionally supported by the European Union Laser Facility Access Program, Contract N° HPRI-CT-1999-00010, the UK Engineering and Physical Sciences Research Council and the "Femto Program" of the European Science Foundation.

References

[1] S. Atzeni, "Inertial fusion fast ignitor: igniting pulse parameter window versus the penetration depth of the heating particles and the density of the precompressed fuel," *Phys. of Plasmas* **6** 3316-3326 (1999).

[2] K. Yasuike, M.H. Key, S.P. Hatchett, R.A. Snavely, and K.B. Wharton, "Hot electron diagnostic in a solid laser target by K-shell lines measurement from ultraintense laser-plasma interactions (3×10^{20} W/cm^2, $\leq$400 J)," *Rev. Sci. Instrum.* **72**, 1236-1240 (2001).

[3] R. Kodama, H. Shiraga, K. Shigemori, Y. Toyama, S. Fujioka, H. Azechi, H. Fujita, H. Habara, T. Hall, Y. Izawa, T. Jitsuno, Y. Kitagawa, K.M. Krushelnick, K.L. Lancaster, K. Mima, K. Nagai, M. Nakai, H. Nishimura, T. Norimatsu, P.A. Norreys, S. Sakabe, K.A. Tanaka, A. Youssef, M. Zepf, and T. Yamanaka, "Fast heating scalable to laser fusion ignition," *Nature* **418**, 933-934 (2002).

[4] R.B. Stephens, R.A. Snavely, Y. Aglitskiy, F. Amiranoff, C. Andersen, D. Batani, S.D. Baton, T. Cowan, R.R. Freeman, T. Hall, S.P. Hatchett, J.M. Hill, M.H. Key, J.A. King, J.A. Koch, M. Koenig, A.J. MacKinnon, K.L. Lancaster, E. Martinolli, P. Norreys, E. Perelli-Cippo, M. Rabec Le Gloahec, C. Rousseaux, J.J. Santos, and F. Scianitti, "K_α fluorescence measurement of relativistic electron transport in the context of fast ignition," *Phys Rev E* **69**, 066414 (2004).

[5] H.-K. Chung, W.L. Morgan, and R.W. Lee, "FLYCHK: an extension to the K-shel spectroscopy kinetics model FLY," *J. Quant. Spect. & Rad. Transf.* **81** (107-115 (2003).

[6] R. Kodama, Y. Sentoku, Z.L. Chen, G.R. Kumar, S.P. Hatchett, Y. Toyama, T.E. Cowan, R. Freeman, J. Fuchs, Y. Izawa, M.H. Key, Y. Kitagawa, K. Kondo, T. Matsuoka, H. Kakamura, M. Kakatsutsumi, P.A. Norreys, T. Norimatsu, R.A. Snavely, R.B. Stephens, M. Tampo, K.A. Tanaka, and T. Yabuuchi, "Plasma devices to guide and collimate a high density of MeV electrons," *Nature* **432**, 1004 (2004).

[7] H.M. Milchberg, R.R. Freeman, S.C. Davey, and R.M. More, "Resistivity of a simple metal from room temperature to 10^6 K," *Phys. Rev. Lett.* **61** 2364-2367 (1988).

[8] M.H. Key, M.D. Cable, T.E. Cowan, K.G. Estabrook, B.A. Hammel, S.P. Hatchett, E.A. Henry, D.E. Hinkel, J.D. Kilkenny, J.A. Koch, W.L. Kruer, A.B. Langdon, B.F. Lasinski, R.W. Lee, B.J. MacGowan, A. MacKinnon, J.D. Moody, M.J. Moran, M.S. Singh, M.A. Stoyer, M. Tabak, G.L. Tietbohl, M. Tsukamoto, K. Wharton, and S.C. Wilks, "Hot electron production and heating by hot electrons in fast ignitor research," *Phys. of Plasmas* **5** 1966-1972 (1998).